Downloaded from orbit.dtu.dk on: Jan 23, 2019

DTU Library

Equal-potential interpretation of electrically induced resonances in metamaterials

Peng, Liang; Mortensen, N. Asger

Published in:
New Journal of Physics

Link to article, DOI:
10.1088/1367-2630/13/5/053012

Publication date:
2011

Document Version
Publisher's PDF, also known as Version of record

Link back to DTU Orbit

Citation (APA):
Peng, L., & Mortensen, N. A. (2011). Equal-potential interpretation of electrically induced resonances in metamaterials. New Journal of Physics, 13(5), 053012. DOI: 10.1088/1367-2630/13/5/053012

General rights
Copyright and moral rights for the publications made accessible in the public portal are retained by the authors and/or other copyright owners and it is a condition of accessing publications that users recognise and abide by the legal requirements associated with these rights.

- Users may download and print one copy of any publication from the public portal for the purpose of private study or research.
- You may not further distribute the material or use it for any profit-making activity or commercial gain
- You may freely distribute the URL identifying the publication in the public portal

If you believe that this document breaches copyright please contact us providing details, and we will remove access to the work immediately and investigate your claim.

IOPscience iopscience.iop.org

Home Search Collections Journals About Contact us My IOPscience

Equal-potential interpretation of electrically induced resonances in metamaterials

This article has been downloaded from IOPscience. Please scroll down to see the full text article.

2011 New J. Phys. 13 053012

(http://iopscience.iop.org/1367-2630/13/5/053012)

View the table of contents for this issue, or go to the journal homepage for more

Download details:
IP Address: 192.38.67.112
The article was downloaded on 11/05/2011 at 09:04

Please note that terms and conditions apply.

New Journal of Physics
The open-access journal for physics

Equal-potential interpretation of electrically induced resonances in metamaterials

L Peng and N A Mortensen
Department of Photonics Engineering, Technical University of Denmark, DTU-Building 345 West, DK-2800 Kongens Lyngby, Denmark
E-mail: plia@fotonik.dtu.dk

New Journal of Physics **13** (2011) 053012 (9pp)
Received 15 December 2010
Published 9 May 2011
Online at http://www.njp.org/
doi:10.1088/1367-2630/13/5/053012

Abstract. We propose a general description of electrically induced resonances (EIR) in metamaterials (MMs) comprising subwavelength unit cells. Based on classical electrodynamics, we found that EIR is governed by an equal-potential effect. Our theory accounts for the EIR phenomena and can give a renewed definition of the effective electric field and hence effective permittivity for MMs made of either dielectrics or metals as well as combinations thereof. The EIR, inherent to the periodic structures, may be the unifying origin of recently observed anomalous electromagnetic phenomena, e.g. the enhanced transmission, the suppressed transmission and the enhanced absorption by a variety of metal film structures in the terahertz range.

Contents

© IOP Publishing Ltd and Deutsche Physikalische Gesellschaft

1. Introduction

The scalar potential is a key concept that has allowed physicists and engineers to understand and interpret a variety of electromagnetic (EM) phenomena [1], yet its strength in the context of metamaterials (MMs) remains unrevealed. In the design and fabrication of MMs, metallic structures are successfully being applied in the microwave range [2]–[4]. At the same time, rod-type structures made of dielectrics with a large permittivity have also been suggested as another route potentially applied in the terahertz and optical range [5]–[7], although some metallic structures are still being applied in the terahertz range [8, 9]. Although these two classes of MMs can realize similar macroscopic EM responses such as anomalous effective permittivity, they do not seem connected due to the apparent different theory bases and design methodologies, which indicates that the common physics behind the MMs still needs to be revealed. In order to clearly advance our fundamental understanding of those EM phenomena in MMs, a unifying theoretical description is essential. The scalar potential offers an attractive solution to this challenge.

To appreciate the common physics of the two classes of MMs, consider first the quasi-static EM response of mixtures of sub-wavelength dielectric particles. An external electric field $\boldsymbol{E}_s$ will polarize the particles, see figure 1(a). The effective permittivity is normally accounted for by the classical Maxwell Garnett (MG) or Clausius–Mossotti (CM) theory [10, 11], with the inherent assumption of only a weakly localized electric field and the absence of resonances [12]. However, in MMs, resonances in the unit-cell structure are critical in making the whole composite possess peculiar EM responses, such as negative ϵ and μ [2]–[4], [13]. In the presence of resonances, a strongly localized field is excited inside the single unit-cell, thus potentially challenging the use of MG or CM theory. As an alternative, more elaborate field-averaging techniques have been used widely to extract effective material parameters [3, 5], [14]–[18], but methods of this kind may lack a solid foundation beyond the static limit and in particular in resonances, i.e. the fields vary rapidly on the scale of the MM unit-cell.

In this paper, we employ an electrical potential approach and propose the electrically induced resonances (EIR) as the unifying concept of MMs made of either dielectrics or metals.

2. Theory

Metallic and dielectric particles may seem to have quite different EM properties, yet their polarizations are similar. In general, for an isolated particle much smaller than the wavelength of light, its polarization is dipole like. The macroscopic dipole moment of particles with positive or negative permittivity (ϵ_{p}) is similar if [1]: (i) the operation frequency is far away from the inclusions' plasma frequency, i.e. $\epsilon'_{\mathrm{p}} \ll -1$ or $\epsilon'_{\mathrm{p}} \gg 1$, or (ii) no magnetic resonance occurs, see figure 1(b).

Consider next an MM made of sub-wavelength structures, generically shown in figure 1(c). All the unit-cell structures are assumed identical and periodically arranged, with incident field ($\boldsymbol{E}_{\mathrm{i}}$) along one axis of the unit cell (z-direction). In resonances, strongly localized electric and magnetic fields are excited inside the unit cell. Although the polarized charges and currents may occupy the entire unit cell and make the problem complex, $\nabla \cdot \boldsymbol{B} = 0$ holds everywhere in space. The Maxwell equations may thus conveniently be rewritten in terms of the scalar potential ϕ and the vector potential $\boldsymbol{A}$ [1], i.e. $\boldsymbol{B} = \nabla \times \boldsymbol{A}$ and $\boldsymbol{E} = -\nabla\phi + \mathrm{i}\omega\boldsymbol{A}$. We emphasize that the distribution of electric and magnetic fields is identical inside each unit cell of an ordered MM,

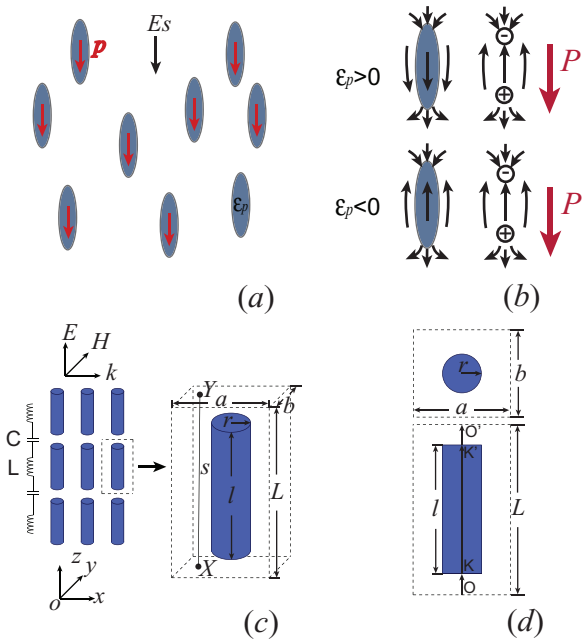

Figure 1. (a) Dilute mixture of sub-wavelength particles. The red arrows indicate the direction of polarization. (b) Schematics of polarization, contrasting different signs of permittivity. The black arrows represent the E-field direction. $\epsilon_{\mathrm{p}} = \epsilon'_{\mathrm{p}} + \mathrm{i}\epsilon''_{\mathrm{p}}$ is the relative dielectric constant of the particle. (c) Schematic diagram of rod-type MM and the corresponding equivalent circuit model. (d) Top and side views of a single unit-cell.

which follows from the Bloch theorem in the $k_0 a \ll 1$ limit. Conceptually, this allows us to focus attention on a single unit-cell [2].

Suppose that a fictitious electron moves from point X (on the bottom surface of the unit cell) to point Y (on the top surface) along path $\boldsymbol{s}$, see figure 1(c). From energy conservation, the work done by the EM force equals the change in the electron's potential energy and

$$-\int_X^Y \nabla\phi \cdot \mathrm{d}\boldsymbol{s} = \phi_X - \phi_Y = \int_X^Y [\boldsymbol{E}(\boldsymbol{s}) - \mathrm{i}\omega \boldsymbol{A}(\boldsymbol{s})] \cdot \mathrm{d}\boldsymbol{s}. \tag{1}$$

Because the $\boldsymbol{E}$ term is of capacitive nature while the $\boldsymbol{A}$ term (determined by the magnetic field) has an inductive origin, we may phenomenologically consider a simplified L–C series equivalent circuit for the MMs, see figure 1(c). To account for MMs made of lossy material, an extra series resistor may be included in the circuit. Note that for a given MM, different polarizations of the incident wave may make the L and C different; thus the resonant frequency shifts.

2.1. The electrostatic case

In solving (1), we first address the electrostatic limit before discussing the general case. For $\omega \to 0$, the gradient of the scalar potential clearly relates only to the electric field. The integration path $\boldsymbol{s}$ could be arbitrary, but the effective electric field on $\boldsymbol{s}$ defined as $\boldsymbol{E}_{\mathrm{eff}} = \hat{s}(\phi_X - \phi_Y)/S$ with S being the total length from X to Y will depend on the choice of $\boldsymbol{s}$. For the given

polarization shown in figure 1(c), the MM's macroscopic electric response is then determined by the potential difference between X and Y. In particular, if $\phi_X = \phi_Y$, the unit cell will behave as an equal-potential body, hence supporting no effective electric field in total. Of course, this is strictly possible only inside a perfect electric conductor (PEC). However, for sufficiently good conductors we may still have $\phi_X \approx \phi_Y$, which turns out to be a central requirement for the existence of the equal-potential effect.

2.2. The general electromagnetic case

Now, we proceed to the more general case of a non-zero frequency. Since the change in energy can be accounted for by considering the potential difference experienced by the fictitious charge, the macroscopic effective electric field should still be expressed as $\boldsymbol{E}_{\text{eff}} = \hat{s}(\phi_X - \phi_Y)/S$. For the common MMs, although the integration path in (1) could be arbitrary, the $\boldsymbol{E}_{\text{eff}}$ can help in reflecting the MM's macroscopic EM effect only when $S = L$, with L being the height of the unit cell, see figure 1(c). For the regularly shaped resonant structures with rotational symmetry, see figure 1(c), the scalar potential is uniformly distributed on the periodically arranged unit-cells' bottom and top surfaces. Thus, from a macroscopic point of view, the effective electric field of the entire unit cell would be evaluated by the potential difference between the top and bottom surfaces, i.e. $\boldsymbol{E}_{\text{eff}} = \hat{z}(\phi_X - \phi_Y)/L$. Meanwhile, the effective electric displacement in a single unit-cell can also be found by taking the polarization into account, i.e. $\boldsymbol{D}_{\text{eff}} = \epsilon_0 \boldsymbol{E}_{\text{eff}} + \boldsymbol{P}_{\text{eff}}$. We emphasize that zero value of $\Delta\phi = \phi_X - \phi_Y$ (and consequently $\boldsymbol{E}_{\text{eff}}$) may also arise in the presence of a finite vector potential's contribution, which often occurs in MMs. The strong dispersion of effective permittivity of MMs occurs close to those frequencies at which the equal-potential condition is satisfied, which we show below. Basically, the macroscopic property of a bulk sample made of the MM specified above can be equivalently described through an effective permittivity

$$\epsilon_{\text{eff},z} = \frac{D_{\text{eff},z}}{E_{\text{eff},z}} = \epsilon_0 + \frac{L}{V}\frac{\int_V \hat{z}\cdot\boldsymbol{P}\,\mathrm{d}v}{\Delta\phi} = \epsilon_0 + \frac{\langle \hat{z}\cdot\boldsymbol{P}\rangle}{\langle\Delta\phi\rangle}, \tag{2}$$

with V being the volume of the unit cell, $\langle \hat{z}\cdot\boldsymbol{P}\rangle = \frac{1}{V}\int_V \hat{z}\cdot\boldsymbol{P}\,\mathrm{d}v$ being the z-component of average polarization and $\langle\Delta\phi\rangle = \frac{\Delta\phi}{L}$ being the average scalar potential difference across the whole unit cell. Again, a strongly dispersive permittivity is apparent when $\phi_X \approx \phi_Y$, and hence anomalous EM responses occur, e.g. in the form of anomalous reflection ($R = |S_{11}|^2$), transmission ($T = |S_{21}|^2$) and enhanced absorption ($A = 1 - R - T$). Here, S_{ij} are the usual components of the scattering matrix.

We should note that here we assume the incident wave to be polarized along the z-direction, which allows us to estimate $\epsilon_{\text{eff},z}$. The MM we study here is in general anisotropic and the other components of $\bar{\epsilon}_{\text{eff}}$ can also be estimated through the same procedure but under some other excitation condition assumption.

3. The effective permittivity of rod-type metamaterials

3.1. Formulation

To further illustrate our points, we consider the example of a periodic cylindrical-rod array, see figure 1(c), with rods of finite length l. In the limit where $l = L$, the rod is effectively infinitely

long. The internal field of the rods $\boldsymbol{E}_{\rm int}$ can conveniently be expressed by the superposition of different-order cylindrical waves [19]. Due to the sub-wavelength scale, high-order cylindrical waves are hardly excited inside a single unit-cell and we have $\boldsymbol{E}_{\rm int}(\rho) \approx \hat{z} E_0 J_0(k_{\rm p}\rho)$ with $k_{\rm p} = \sqrt{\epsilon_{\rm p}}(k)_0$ being the wavenumber inside the rod. Since the scalar potential is uniform on both the bottom and top surfaces, the potential difference can be conveniently determined by (1) with an integration path connecting the bottom center and the top center, i.e. O–O' in figure 1(d). Four points are critical in determining the integration, i.e. O, O', K and K', and formally we have $\phi_X - \phi_Y = V_{OK} + V_{KK'} + V_{K'O'}$ with $V_{OK} = \phi_O - \phi_K$, $V_{KK'} = \phi_K - \phi_{K'}$ and $V_{K'O'} = \phi_{K'} - \phi_{O'}$. The three terms can be worked out by interpreting the electrodynamics inside the unit cell. Since the polarization current flows along the cylinder but the polarization charge mainly distributes on the two ends, it is natural to assume that the scalar potential inside the cylinder, i.e. close to the straight line K–K', is related to both the electric and magnetic fields. However, close to the straight segments O–K and K'–O', only the instantaneous electric field is involved, since $\boldsymbol{A}$ will be completely canceled by the non-instantaneous component of $\boldsymbol{E}$ in (1) in a source-free case. Having calculated the potential difference, we apply (2) and, after some tedious but straightforward algebra, we finally arrive at

$$\epsilon_{\rm eff,z} = \epsilon_0 \left\{ 1 + \frac{2\pi r l J_1(k_{\rm p} r)}{k_{\rm p} a^2 \Delta\phi} \right\} = \epsilon_0 \left\{ 1 + \frac{2f}{\langle \Delta\phi \rangle} \frac{J_1(k_{\rm p} r)}{k_{\rm p} r} \right\}, \tag{3}$$

with $f = \frac{\pi r^2 l}{a^2 L}$ being the volume fraction, $\langle \Delta\phi \rangle = \frac{\Delta\phi}{L}$ being the average scalar potential difference and

$$\Delta\phi = \left(\frac{2\epsilon_{\rm p} - 1}{\epsilon_{\rm p} - 1} \right) \frac{l}{\epsilon_{\rm p}} + \frac{l}{\epsilon_{\rm p}} \left[k_{\rm p} r J_1(k_{\rm p} r) \ln\left(\frac{r}{R} \right) - J_0(k_{\rm p} r) \right] + \Phi(0) - \Phi(l) - \Phi\left(\frac{L-l}{2} \right) + \Phi\left(\frac{L+l}{2} \right). \tag{4}$$

Here, $R = a/\sqrt{\pi}$ and $\Phi(d) = \int_0^r \frac{J_0(k_{\rm p}\rho)}{\sqrt{\rho^2 + d^2}} \rho \, {\rm d}\rho$. Note that our theoretical analysis is general and can equally well describe the effective permittivity of MMs made of either dielectrics ($\epsilon_{\rm p}' > 0$) or metals ($\epsilon_{\rm p}' < 0$). Resonances are expected when $\Delta\phi \approx 0$.

3.2. Numerical evaluation

In the following, we numerically explore the consequences of (3). Firstly, we consider dielectric cylinders. Figure 2(a) shows the effective permittivity calculated with the aid of (3), the parameters of which are explained in the figure caption. As seen, the MM composed of ILR possesses a strongly dispersive effective permittivity, in full agreement with results in [5]–[7]. When turning to rods of finite length, the EIR is shifted towards higher frequencies and the effective permittivity exhibits almost no frequency variation in the considered frequency range, see the dashed line in figure 2(a). Due to the absence of resonance in the close frequency vicinity, the nearly non-dispersive $\epsilon_{\rm eff}$ can here equally well be interpreted by MG or CM theory.

Secondly, we turn to cylinders made from a dispersive media whose permittivity obeys a Lorentz model in the terahertz region, i.e. $\epsilon_{\rm p} = 1 - \omega_{\rm p}^2/(\omega^2 - \omega_0^2)$ with plasma frequency $\omega_{\rm p}/2\pi = 600\,{\rm THz}$ and binding frequency $\omega_0/2\pi = 200\,{\rm THz}$. The dimensions of the MM unit-cell are now scaled down to nano size, as specified in the caption of figure 2(b). As seen from the results, the MM made of infinitely long cylinders will preserve the binding frequency

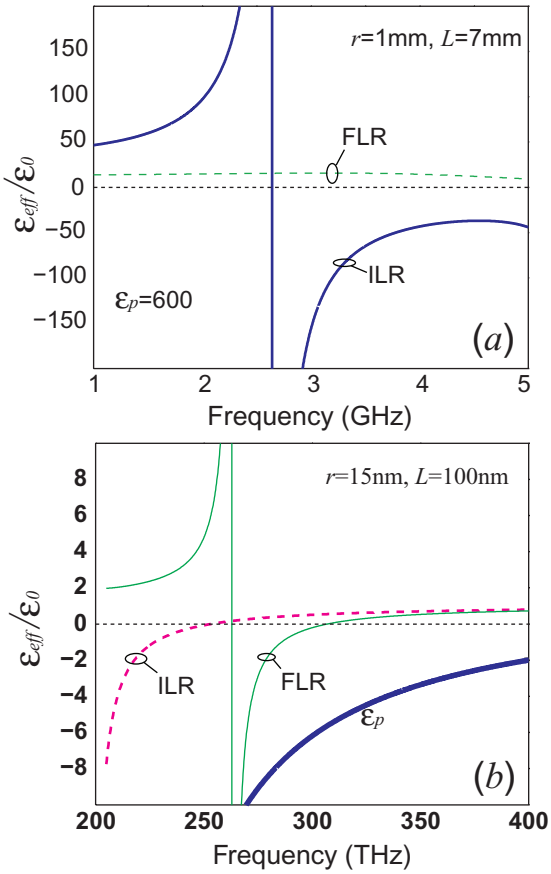

Figure 2. Effective permittivity ϵ_{eff} for a rod-type MM with a cubic unit-cell. (a) Dielectric rods with $\epsilon_{\text{p}} = 600$, $r = 1\,\text{mm}$ and $L = 7\,\text{mm}$ with the results contrasting infinitely long rods (ILR) with finite-length rods (FLR) ($l = 6.95\,\text{mm}$). (b) Rods supporting a dispersive plasma with $r = 15\,\text{nm}$ and $L = 100\,\text{nm}$ with the results contrasting ILR with FLR ($l = 80\,\text{nm}$).

while having an effective plasma frequency much smaller than that of the original plasma media, as previously predicted [2]. However, for the MM comprising cylinders of finite length, the effective permittivity is strongly dispersive with both the effective plasma frequency and the binding frequency are modified. Clearly, figures 2(a) and (b) display the same qualitative Lorentz-like behavior (compare blue and green curves), thus emphasizing the common physics of the two MM classes.

4. Extraordinary transmission, suppressed transmission and enhanced absorption

4.1. The gold rod array

As shown above, our theory can successfully be used to describe the MMs, both dielectric and metallic. However, its application is not restricted to infinite stacks of MM unit-cells. If only a single layer of MM unit-cells exists, equation (2) cannot immediately be applied, but the MM

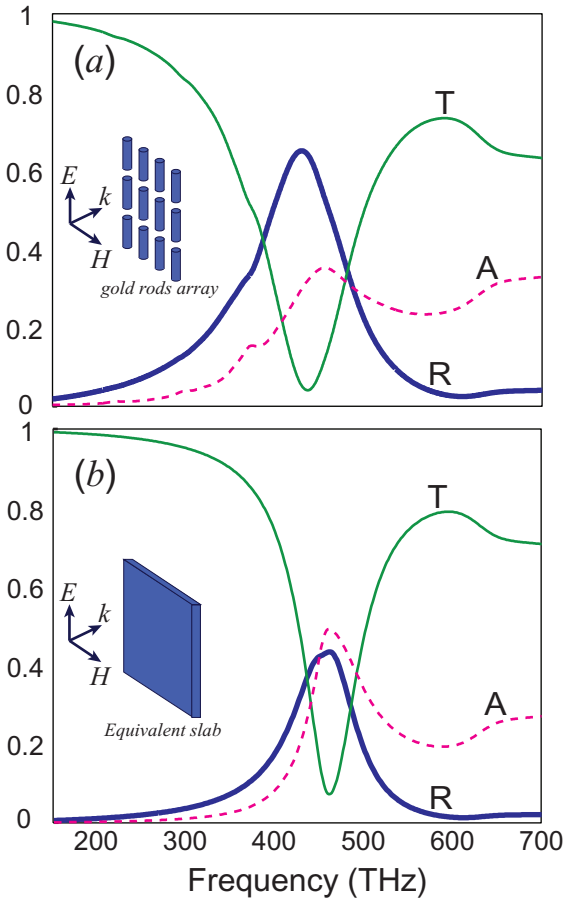

Figure 3. Full-wave simulations of the EM response of a gold-rod array with $L = 100\,\text{nm}$, $r = 15\,\text{nm}$ and $l = 80\,\text{nm}$. (a) Results resolving the detailed MM unit-cell structure. (b) Results for the homogenized MM slab with effective permittivity derived from equation (3). Since equation (3) is basically not applied to this one-layer composite, hence, the two curves shown cannot perfectly match. In the simulation, the incident plan wave propagates along the $\hat{x}$-direction, with polarization along the $\hat{z}$-direction, see figure 1(c). Only a single unit-cell is placed into the simulation site, with periodic boundary conditions being applied in the in-plane ($\hat{y}$ and $\hat{z}$) direction.

still exhibits EIR behavior, which is also plasmon like in the terahertz range, i.e. anomalous reflection together with strong absorption. To illustrate this, we take an MM made of finite gold rods as an example. The unit-cell is quadratic with lattice constant $L = 100\,\text{nm}$ and the gold rods have radius $r = 15\,\text{nm}$ and length $l = 80\,\text{nm}$. For the dielectric constant of gold, see [20]. In figure 3(a), a full-wave simulation of the one-layer MM clearly reveals a resonance around 460 THz at which strong reflection and absorption occur and consequently the transmission is low. Figure 3(b) shows corresponding results for an effective medium slab with a permittivity derived from (3). Note the qualitative agreement between panels (a) and (b).

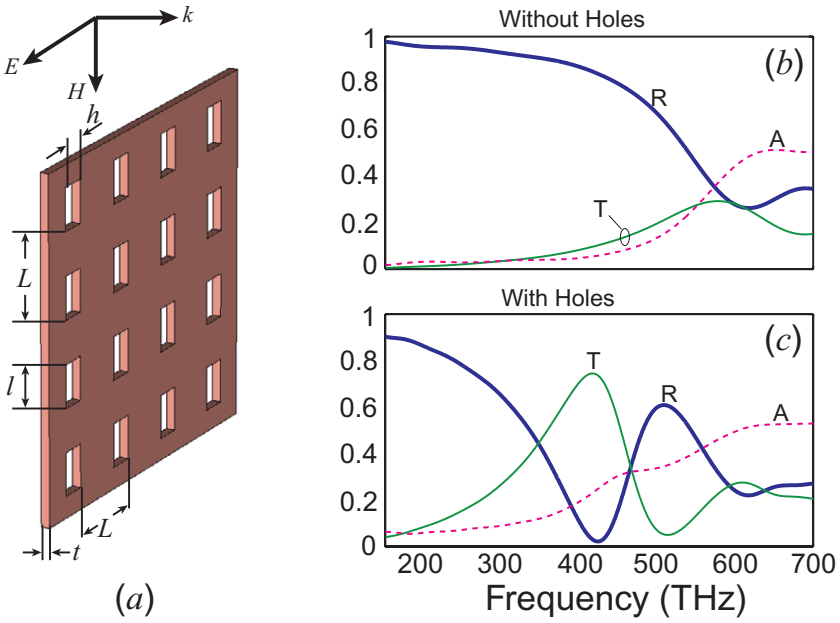

Figure 4. (a) Gold thin film with $t = 30\,\text{nm}$, $l = 75\,\text{nm}$, $h = 12\,\text{nm}$ and $L = 100\,\text{nm}$. (b) Full-wave simulations of the EM response in the absence of any holes. (c) The corresponding response in the presence of an air-hole array. Still, in the simulation there is one unit-cell in the $\hat{k}$-direction and periodic boundary condition applied in the in-plane directions. The unit-cell length in the $\hat{k}$-direction is L.

4.2. Ultrathin gold film with a subwavelength hole array

Figures 2 and 3 present typical examples of MMs displaying resonances with our new theory offering an equal-potential description. However, our theory applies to MMs beyond the rod-type structures emphasized so far. In fact, the EIR discussed here occurs in most MMs comprising periodically arranged sub-wavelength structures, including fish-net structures and arrays of sub-wavelength holes in thin metal films. As an example, figure 4(a) considers a semi-transparent 30 nm thick (comparable to the skin depth at 460 THz) gold film with a periodic array of holes. The detailed parameters employed in the simulation are listed in the caption. The film investigated resembles the inverse structure of the rod array studied in figure 3(a), and from Barbinet's principle, we expect it to exhibit similar EM behavior. Formally, the film's qualitative EIR behavior may also be addressed by our equal-potential description, but analytical calculations resembling (3) are too complex and results are not included. However, our full-wave simulations clearly show the appearance of the anticipated resonance appearing around $\omega_0/2\pi = 460\,\text{THz}$, see figure 3(c). For comparison, figure 3(b) shows the corresponding results for a closed gold film, where the absence of holes prevents extraordinary transmission (accompanied by suppressed reflection) below ω_0 and suppressed transmission above ω_0.

5. Conclusion

In conclusion, a new description of EIR has been established with the help of the scalar potential. Originating from classical electrodynamics, our theory accounts well for MMs made of either dielectrics or metals and could be expanded to describe an arbitrary composite of subwavelength structures. The theory presented establishes the relationship between the equal-potential effect and the EIR, which also helps in interpreting recently reported phenomena, such as extraordinary transmission, suppressed transmission and enhanced absorption by MMs and periodic structures [21]–[25]. Our unified potential description may stimulate more use of dielectric structures to mimic desired properties readily achieved with more lossy metallic counterparts.

Acknowledgments

We thank S Xiao, M Wubs and W Yan for discussions. This work was financially supported by the *Danish National Advanced Technology Foundation* (grant no. 004-2007-1).

References

[1] Jackson J D 1999 *Classical Electrodynamics* 3rd edn (Hoboken, NJ: Wiley)
[2] Pendry J B, Holden A J, Stewart W J and Youngs I 1996 *Phys. Rev. Lett.* **76** 4773
[3] Pendry J B, Holden A J, Robbins D J and Stewart W J 1999 *IEEE Trans. Microw. Theory Tech.* **47** 2075
[4] Chen H, Ran L, Huangfu J, Zhang X, Chen K, Grzegorczyk T M and Kong J A 2004 *Phys. Rev.* E **70** 057605
[5] Peng L, Ran L, Chen H, Zhang H, Kong J A and Grzegorczyk T M 2007 *Phys. Rev. Lett.* **98** 157403
[6] Vynck K, Felbacq D, Centeno E, Căbuz A I, Cassagne D and Guizal B 2009 *Phys. Rev. Lett.* **102** 133901
[7] Peng L, Ran L and Mortensen N A 2010 *Appl. Phys. Lett.* **96** 241108
[8] Singh R, Azad A K, O'Hara J F, Taylor A J and Zhang W 2008 *Opt. Lett.* **33** 1506
[9] Singh R, Smirnova E, Taylor A J, O'Hara J F and Zhang W 2008 *Opt. Express* **16** 6537
[10] Maxwell Garnett J C 1904 *Phil. Trans. R. Soc.* **203** 385–420
[11] Sihvola A 1999 *Electromagnetic Mixing Formulas and Applications (IEE Electromagnetic Waves Series 47)* (Stevenage, Herts, UK: The Institution of Electrical Engineers)
[12] Ruppin R 1978 *Phys. Status Solidi* B **87** 619–24
[13] Smith D R, Padilla W J, Vier D C, Nemat-Nasser S C and Schultz S 2000 *Phys. Rev. Lett.* **84** 4184
[14] Smith D R and Pendry J B 2006 *J. Opt. Soc. Am.* B **23** 391
[15] Silveirinha M G 2007 *Phys. Rev.* B **76** 245117
[16] Silveirinha M G 2007 *Phys. Rev.* B **75** 115104
[17] Cerdán-Ramírez V, Zenteno-Mateo B, Sampedro M P, Palomino-Ovando M A, Flores-Desirena B and Pérez-Rodríguez F 2009 *J. Appl. Phys.* **106** 103520
[18] Ortiz G P, Martínez-Zérega B E, Mendoza B S and Mochán W L 2009 *Phys. Rev.* B **79** 245132
[19] Tsang L, Kong J A and Ding K H 2000 *Scattering of Electromagnetic Waves: Theories and Applications* (New York: Wiley)
[20] Johnson P B and Christy R W 1972 *Phys. Rev.* B **6** 4370
[21] Ebbesen T W, Lezec H J, Ghaemi H F and Thio T 1998 *Nature* **391**
[22] Braun J, Gompf B, Kobiela G and Dressel M 2009 *Phys. Rev. Lett.* **103** 203901
[23] Xiao S, Zhang J, Peng L, Jeppensen C, Malureanu R, Kristensen A and Mortensen N A 2010 *Appl. Phys. Lett.* **97** 071116
[24] Landy N I, Sajuyigbe S, Mock J J, Smith D R and Padilla W J 2008 *Phys. Rev. Lett.* **100** 207402
[25] Liu X, Starr T, Starr A F and Padilla W J 2010 *Phys. Rev. Lett.* **104** 207403